

A SURVEY OF GEOSYNCHRONOUS SATELLITE GLINTS

Frederick J. Vrba, Michael E. DiVittorio

U.S. Naval Observatory, Flagstaff Station

10391 W. Naval Observatory Road, Flagstaff, AZ 86001

Robert B. Hindsley, Henrique R. Schmitt, J. Thomas Armstrong

Naval Research Laboratory, Remote Sensing Div. Code 7210

4555 Overlook Ave., SW, Washington, DC 20375

Paul D. Shankland, Donald J. Hutter, and James A. Benson

U.S. Naval Observatory, Flagstaff Station

10391 W. Naval Observatory Road, Flagstaff, AZ 86001

ABSTRACT

We present USNO Flagstaff Station optical photometric measurements from an intense campaign to monitor geosynchronous satellite glints in support of interferometric measurements at the Navy Prototype Optical Interferometer (NPOI). While observations were obtained during four glint seasons over two years, we concentrate here on observations from the vernal equinox 2009 glint season. In particular, 8 consecutive nights of photometry were obtained of DirecTV-9S which show the evolution of glints from that satellite. This is of particular interest since interferometric fringes were obtained at NPOI during two of these nights. We discuss the timing, shapes, and durations of the glints along with notional glint models. We also briefly discuss glints from other satellites in the constellation surrounding DirecTV-9S; GE-2, GE-4, and DirecTV-4S.

1. INTRODUCTION

During the past decade numerous optical photometric studies of on-orbit geosynchronous (geosats) and semi-geosynchronous satellites have been carried out. These studies show that many details about these satellites can be obtained from their reflected light intensity and color signatures as the Solar-Vehicle-Observer (SVO) illumination (or phase) angle changes such as: aging [1], material properties [2,3], shape classes [4], solar panel offsets [4], and change analysis [5]. Enough data and analyses have now been obtained that even individual satellites can be identified from their photometric signatures [5,6]. Most of these analyses are based on monitoring of the primarily-Solar diffuse reflected light off the spacecraft, which dominates most of the phase angle signatures. However, at times of favorable alignment between the satellite, observer and Sun, specular reflection off of relatively flat surfaces, such as solar panels, can cause brief but spectacular increases in reflected light over that of the nominal diffuse signature. Such events, commonly referred to as "glints", have been observed ubiquitously for Iridium satellites [7] and often for GPS satellites [1] and, geosats [8]. In the case of geosats, the most favorable SVO glint angle of 0 degrees is precluded by Earth shadow, as are all Solar-Vehicle-Earth (SVE) angles of less than approximately 8.5 degrees, as the Earth's shadow is approximately 17 degrees at geosat altitude (approximately 37500 km) and causes an eclipse season of about 45 days centered on each equinox. Thus, much of the potential glint information is usually lost. The data in fig. 1 are typical of this situation wherein optical photometry from the U.S. Naval Observatory, Flagstaff Station (NOFS) of Telstar 6 shows a nominal "Telstar" geosat signature class as defined by [4], but interrupted for more than one hour (or +/-8.5 degrees of SVE phase angle) as the satellite passed through Earth shadow. Potential information from the light curve at lower SVE phase angles is simply lost.

Nonetheless, significant geosat glints can also be observed at minimum SVO angle just outside Earth eclipse when the apparent declination of the satellite is near that of the Sun. As seen from the Flagstaff Station of USNO (NOFS) most geosats have apparent declinations of somewhat less than -5 degrees providing a glint season centered about 3 weeks after Autumnal Equinox and 3 weeks before Vernal Equinox. This is abetted by the fact that geosynchronous communication satellites are equipped with over-sized solar panels which are often not pointed normal to the Sun during early years of operation, effectively shifting the glint geometry in time to being outside of Earth shadow. While observations exist in the literature which note the peak brightnesses, durations, and phase angles of several individual glints, to our knowledge, no extended study of geosat glint characteristics exists previous to the work reported here.

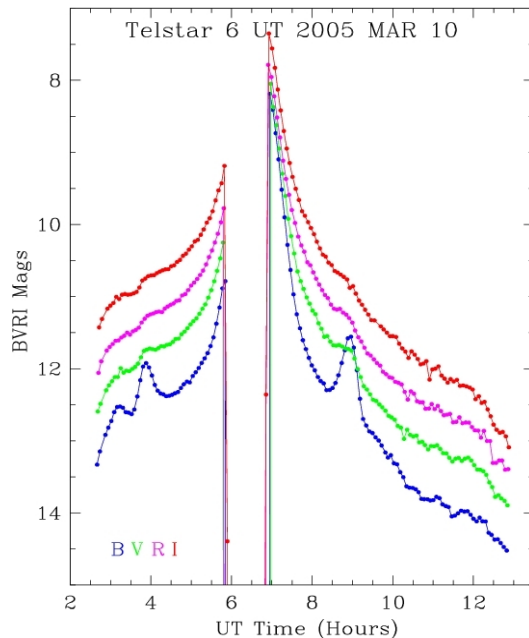


Fig. 1. BVRI photometric observations of Telstar 6 on UT 2005 Mar 10

2. NOFS/NPOI OBSERVATIONS

Beginning in the fall of 2007 an effort was initiated at the Navy Prototype Optical Interferometer (NPOI) [9], located at Anderson Mesa approximately 11 miles SE of NOFS, to obtain interferometric fringes of geosynchronous satellites. The observation limit for interferometric imaging at NPOI is approximately 6th magnitude, well above the typical apparent brightness of geosats outside of a glint. Thus, all efforts were directed toward observing geosats during the four glint seasons of fall 2007, spring 2008, fall 2008, and spring 2009, each of 7 to 9 nights in duration.

A significant problem to overcome was that NPOI needed astrometric positions of the geosats to approximately ± 1 arcsec in order to search for fringes in a reasonable amount of time, but the available two line element sets (TLEs) are not accurate at this level and the geosats are not brighter than 6th magnitude long enough for NPOI to perform astrometry. Thus, it was decided to use the 40-inch Ritchey telescope at NOFS to provide near-real time observations of the geosats chosen to be observed. While the 40-inch telescope is not *per se* an astrometric telescope, multiple exposures of a geosat field with the telescope tracking turned off gives sufficient astrometric accuracy, given a large enough field of view and short exposure times to get multiple short reference star trails. An additional problem is that, even for geosats with low inclination orbits, apparent motions of one to two minutes of arc over a few hours are not uncommon. Thus, an aggressive program was developed of monitoring several satellites each night to obtain sufficient time-coded astrometry in order to make predictions of the geosats' altitude and azimuth as seen from NPOI at the time of predicted glint; often predicting positions for expected times exiting Earth's shadow. After overcoming initial start-up and weather problems early on, a breakthrough came with a probable fringe detection of DirecTV-9S during the spring 2008 run [10] followed by highly certain fringe detections of DirecTV-9S on two separate nights during the spring 2009 run [11,12]. Details of the interferometric measurements and physical implications are given in [11,12].

While the primary purpose of the NOFS 40-inch observations was to obtain support astrometry for NPOI, a residual benefit is a large set of CCD observations of a variety of geosats during the four glint seasons. While a significant fraction of these observations were obtained through non-photometric and/or poor seeing conditions there is also a subset of photometrically-calibrated observations, most of which have not yet been analyzed. Amongst the geosats observed were: Anik-F1, Anik-F1R, DirecTV-4S, DirecTV-7S, DirecTV-9S, Echostar-5, Echostar-10, Echostar-11, Galaxy-10R, Galaxy-12, Galaxy-14, Galaxy-15, Galaxy-18, Galaxy-21, GE-2(AMC-2), and GE-4(AMC-4). If there is sufficient community interest more of these data could be reduced and analyzed.

Our discussion here will be limited to the results for DirecTV-9S (hereafter DTV-9S) and its constellation companion satellites during the spring 2009 observing season, GE-2(AMC-2), GE-4(AMC-4), and DTV-4S, not only because of the successful interferometric observations of DTV-9S, but because of the intensity of observations during an eight night period from (UT) 2009 February 25 through March 04. All observations were obtained with the NOFS 40-inch telescope using a 2048x2048 LN2-cooled Tektronics CCD covering a field of approximately 22x22 arcmin with 0.68 arcsec pixelization. Observations were normally taken through a standard R filter or, when the satellites became bright, through a narrow-band H-alpha filter of approximately the same effective wavelength to avoid saturation. The relative throughput between the R and H-alpha filters is well-calibrated such that observations across filter changes are seamless and we will not distinguish the observations hereafter. While integration times were adjusted between 5.0 and 1.0 seconds, depending on the filter and brightness of the target, the CCD readout time was about 45 seconds, resulting in an effective duty time of roughly 50 seconds. Observations were calibrated to nearby standard stars [13] on photometric nights.

3. THE GE-2, GE-4, DTV-9S, DTV-4S CONSTELLATION

The constellation of geosats containing GE-2, GE-4, DTV-9S, and DTV-4S (hereafter GGDD) is shown in Fig. 2 as a stacked set of R and H-alpha filter images taken on UT 2009-March-02. North is at the top and East to the left and the full 22x22 arcmin field is shown. A total of 154 frames taken over the course of somewhat more than 3 hours is shown. The true brightnesses of the satellites are not shown in this image, as there have been no corrections for exposure times or filter changes. However, this figure demonstrates the large apparent motions of even nominally-orbited geosats over the course of a few hours and thus the need for the astrometric monitoring described above. From East to West the satellites are GE-2, GE-4, DTV-9S, and DTV-4S. This constellation is located at approximately 101degrees West Longitude, placing it at an East Hour Angle of 00h 49m as seen from NOFS.

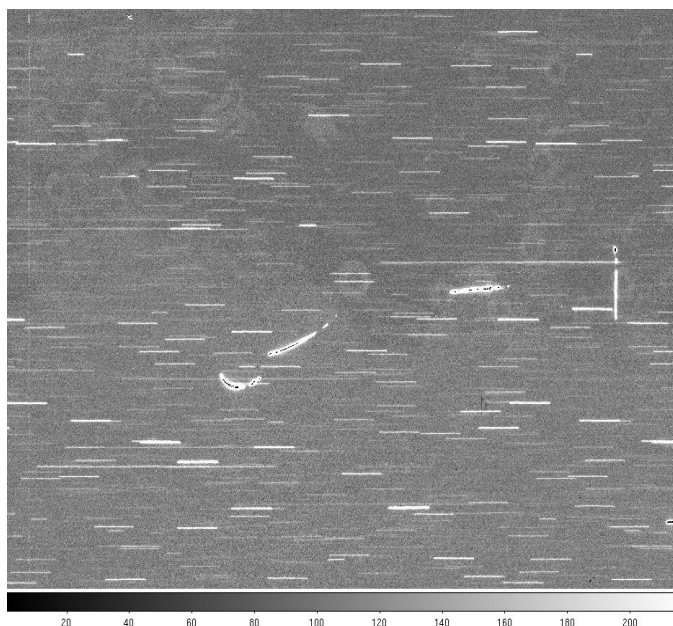


Fig. 2. Stacked R and H-alpha frames of the GGDD geosat constellation taken on UT 2009-March-02

Fig. 3 displays the calibrated R-band photometry of the GGDD constellation obtained on UT 2009-March-02. Because the primary purpose of these observations was astrometry for NPOI, often compromises were made in the photometric observations; in this case a decision to obtain astrometry of a different field after UT 6.6 hours compromised a full measurement of the DTV-4S glint, although this constellation would have soon entered eclipse (see below).

DTV-9S was launched in October 2006 and is a Space Systems/Loral LS-1300 bus; as such it produces a purely “canonical” light curve [4], in this case with a strong glint. The artist's conception from the Loral website shown in Fig. 4 shows no unusual features which would cause a non-canonical signature.

DTV-4S was launched in November 2001 and is a Boeing 601HP bus; as such it is considered a “peculiar” signature class [4]. Evidence for this is in the extremely “noisy” light curve. Whether or not the spacecraft glinted more strongly is lost by the cutoff of photometry.

GE-4 (AMC-4) was launched in November 1999 and is a Lockheed Martin A2100AX bus; as such it has an “A2100” class signature [4]. These satellites have two peaks in their signatures with a local minimum of light at minimum phase angle; completely opposite from “canonical” signatures. This may be due to counter-rotated solar panels. In Fig. 3 we are seeing the first of the two peaks.

GE-2 (AMC-2) was launched in January 1997 and is a Lockheed Martin A2100A bus and is also classified as an “A2100” signature [4]. While the light curve between 3.5 and 5.0 hours is consistent with an A2100 signature, clearly a strong but irregular glint is occurring where there should be a local minimum. The reasons for this are unclear but it may be that one of the panels is glinting while the other panel is rotated enough for only diffuse reflection.

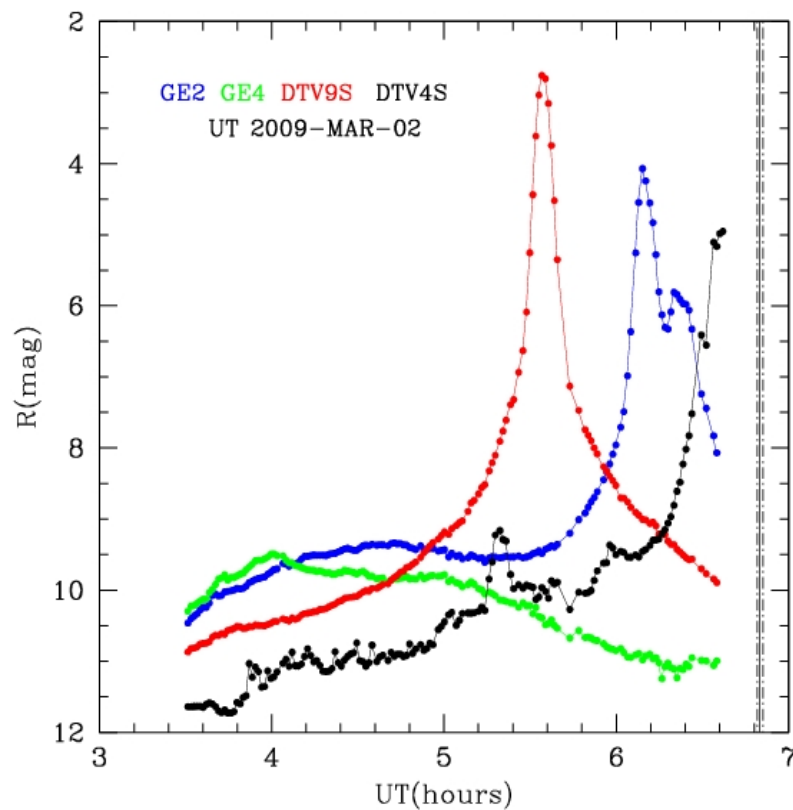


Fig. 3. R-band photometry of the GGDD geosat constellation UT 2009-March-02

The solid line at the far right of Fig. 3 is at the time of minimum SVO phase angle for the center of this constellation on UT March 02: UT 06h 50m with a minimum SVO of 12.6 degrees. However, the SVE of the constellation would have dropped below the eclipse threshold of 8.5 degrees almost immediately after the observations were terminated and further data would have been lost for the duration of the eclipse. The constellation has an extent of about 15 arcmin (Fig. 2), corresponding to a range of minimum SVO times of about +/- 30 seconds shown by the dashed lines at far right (barely discernible). While the light curves for GE-4 and DTV-4S are consistent with the time of minimum SVO (GE-2 is indeterminate in this sense), clearly DTV-9S glinted at a much different time: 1.254 hours earlier, corresponding to 18.8 degrees of phase. This implies that DTV-9S' solar panels were offset from the normal to the Sun by 9.4 degrees to the West. This is well within the range of recorded solar panel offsets [4] and, as noted earlier, is often seen during the early years of geosat operation. The solar panel offset moved the glint far enough in time and phase angle that the peak glint could be observed outside of Earth's shadow. This had the fortunate affect of allowing

observations of the evolution of DTV-9S over several days as discussed in the next section. The offset also foreshortens the solar panel apparent dimension (see Section 5).



Fig. 4. An artist's conception of DTV-9S from the Loral website

4. THE EVOLUTION OF THE DTV-9S GLINTS

Nightly observations of DTV-9S glints started on UT 2009-FEB-25 and went through UT 2009-MAR-04, for a total of 8 nights. Four of the nights were completely photometric (UT 2009-MAR-02, Fig. 2 being an example), two nights were photometric during DTV-9S glints, and for two nights the DTV-9S photometry could be reconstructed from fitting to GE-4 data, which served as a “local standard source”. The results for the UT 5.0 to 6.1 hour period centered on the glints are shown in Fig. 5. The faintest and narrowest glint is from 25 Feb and the glints continue to brighten and widen through 04 Mar with the last three glints appearing to essentially saturate in amplitude and width.

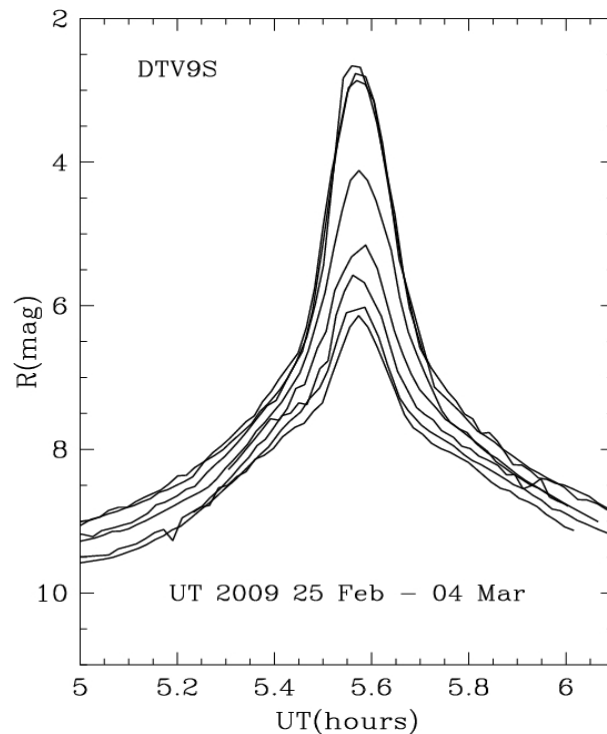


Fig. 5. DTV-9S glints measured on 8 night between UT 2009 February 25 and UT 2009 March 04

What is not obvious in this plot is that the DTV-9S images at peak flux on March 03 are badly saturated, while the DTV-9S images at peak flux on the surrounding days are not saturated. Thus, it appears that we were able to observe the maximum, on March 03, of DTV-9S glints during this glint season, with the expectation that glints on subsequent nights would have been fainter if observations beyond March 04 would have continued. While it is nearly impossible to estimate the actual peak brightness of DTV-9S on March 03 because of the degree of image saturation, it is plausible that the peak was brighter than magnitude +1.

Fitting polynomial functions to the 12 data points surrounding the peak light each night we find the mean peak UT time for the eight nights is UT 5.579 +/- .004 hours. The RMS scatter in the peak times is thus 14 seconds. Recall that our sampling time is about 50 seconds. Assuming Poisson statistics for 12 data points per fit the fundamental time resolution is also 14 seconds. Thus, our sampling time was not sufficient to resolve changes in the evolution of peak time below 14 seconds. Recall also that DTV-9S may have an East-West motion of about 2 arcmin during a night (see Fig. 2) implying an intrinsic distribution of peak times of as much as 8 seconds.

5. DECONSTRUCTING DTV-9S GLINTS

The brightness of an ideal glint can easily be calculated from first principles [7,14]. If we assume that the object reflecting the sun light is a flat mirror, then the light from the object is simply equal to the light from the fraction of the angular area of the sun subtended by the reflector. While the brightness is directly proportional to the size of the reflector, the size of the glint patch striking the earth is almost completely dependent on the angular size of the Sun and is nearly independent of the size of the reflector, unless the reflector is very large (on the order of many tens of kilometers). Since the sun has an angular diameter of $\sim 1/2$ degree, the beam of light coming from the reflecting object will therefore radiate in a cone of light with a divergence of $1/2$ degree. From geosat orbit, such a ground trace will be ~ 320 km in diameter. Such a patch of light would have very steep rise and fall times, with the passing of the projection of the Sun's limb across the observer resulting in a transition time of $\ll 1$ second. The full diameter of the glint would take approximately 2 minutes to pass over the observer. During glint season this patch of light will start in the hemisphere opposite from the Sun and migrate night by night past the equator and into the opposite hemisphere. This is why the geosat glint season is prior to vernal and after the autumnal equinox in the North, and after the vernal and prior to the autumnal equinox in the South. As mentioned in Section 3, the optimum glint alignment takes place during Earth eclipse and therefore in the case of glint from a flat reflector normal to the Sun the glint would not be observable.

The apparent size of the solar arrays on the DTV-9S satellite (approximately 2×30 meters) at geosat distance (37500 km) is approximately $11 \text{ mas} \times 165 \text{ mas}$. Assuming a Solar radius of $16' 08''$ for the dates of the spring 2009 observation (The Astronomical Almanac), an apparent Solar magnitude of -26.73, and still assuming they are acting as a flat mirror with an albedo of 1, we expect a glint with a magnitude of -3.9. Furthermore, as observed from NOFS, when the glint is centered over northern Arizona i.e. the full diameter of the patch of light projected on the Earth passes over, the glint duration should be ~ 2 minutes, with observer aperture dependent rise and fall times; approximately 0.001 second for the NOFS 40-inch telescope.

However, actual glints observed from geosats are typically only as bright as ~ 2 mag and can last as long as 1 hour from initial rise until the object has returned to its nominal diffuse signature (Fig. 3). The glints observed from DTV-9S (Fig. 5) exhibit these same smaller amplitude and wider width characteristics as compared to the ideal glint. Since glints are observed to be not as bright as predicted, but last many times longer, then it is probable that the reflecting objects are, in fact, not optically flat. If the panels are either curved (optically powered) or an array of small flats with different tilts, the patch of reflected light on the earth will be much larger, and the average intensity, and therefore apparent observed magnitude will be fainter.

For example, if the panel is made of a large number of small, flat pieces, each individually tilted, then the beam would be spread out over a larger angle and the glint patch on the Earth would be larger. The full time scale of DTV9-S glints is approximately 1 hour (Fig. 5) as compared to 2 minutes for the ideal glint. This implies an East-West patch size of 30 times the ideal patch of 320 km, and therefore an average flux density of $1/900$ the ideal case. A notional fit, however, to the observed profile and peak magnitude is to assume a conical profile from the peak magnitude (+2.4) down to a characteristic core glint timescale of 0.4 hours. Noting also that the glint flux will be reduced by elongation of the glint beam onto the Earth due to the geosat approximate zenith distance of 40 degrees in the North-South direction we derive a solar panel albedo of 0.09, which compares well with documented albedo values for new solar panels of about 0.12 [2]. As mentioned in Section 4, due to CCD image saturation, the peak glint brightness of

DTV-9S on March 03 was likely significantly brighter than +2.4 magnitude, which would result in a higher calculated albedo. Clearly, more sophisticated models would produce more accurate flux and albedo estimates.

The DTV-9S notional glint time scale of 1 hour would be produced by solar array sub-panels with tilts up to ± 3.75 degree. As observed, the patch of light on the earth will be projected over an angle of 15 degrees (± 7.5 after reflection), and will therefore be 30 times the diameter of the ideal case (1/2 degree). An actual solar panel is likely to have a random distribution of sub-panel alignment errors, most well aligned and fewer with larger error values, producing the Gaussian-like light curves observed in Fig. 5.

Although detailed modeling of glint spot structure based on solar panel models would be necessary, our analysis suggests that by measuring the maximum brightness and calculating the diameter of the glint patch of light projected on the earth, the diffuse nature of a satellite glint may be derived and basic parameters such as area and/or albedo of the reflecting object may be estimated.

6. DISCUSSION AND FUTURE WORK

The significant offset of the DTV-9S solar panels moved its suite of glints well away from Earth shadow eclipse and allowed us to obtain the evolutionary glint results we report in this contribution. Its Hour Angle as seen from Flagstaff also allowed a large amount of time-dependent astrometry to be obtained before its glint time. These combined circumstances, along with fortuitous weather during our campaigns, are likely the main reasons that DTV-9S is the first geosat for which NPOI obtained successful measurements of interferometric fringes [10,11,12]. It is true that DTV-9S has an especially smooth diffuse light signature. Fitting of the data for the geosats shown in Fig. 3 between 4 and 5 hours UT shows RMS scatters of 0.022, 0.028, 0.049, and 0.130 magnitudes for DTV-9S, GE-2, GE-4, and DTV-4s, respectively. Whether this is indicative of an especially stable or smooth-surfaced spacecraft is unknown. However, both the photometric and interferometric results demonstrate that geosat glints are not merely a backyard binocular entertainment, but can provide information on geosats beyond what can be deduced from their diffuse signatures.

In the photometric domain alone our results suggest that the precise timing of geosat glints can provide information on solar panel micro-offsets. We note that even the ± 14 second dispersion of the DTV-9S glint peaks corresponds to ± 0.03 degree panel tilt angle. At this level, implications for spacecraft may become apparent. While detailed modeling of glint spots on the Earth will be necessary, our notional analysis of glint durations and amplitudes leads to an independent method of measuring solar panel albedos. An issue that we did not address in our notional analysis in this paper was that of a proper subtraction of the underlying diffuse light component. While the diffuse component has little affect on peak light (e.g. glint timing) it will have a significant affect on understanding the energy distribution across the entire glint spot. From an observational standpoint, higher photometric time resolution than our 50 second duty cycle is desired and easily obtainable. While our observations in support of NPOI interferometric measurements were constrained in several ways in order to produce the best astrometry, future photometric campaigns should employ telescope, filter, and exposure time combinations which, while providing high S/N results, are designed to not allow the glint images to become saturated. Our observations over multiple nights had the effect of sampling multiple chords through the glint patch as it moved in latitude from night to night. This can also be accomplished by multiple observations of the glint spot on the same night from different latitudes. Multiple observations on different nights and observing latitudes would provide for even higher glint spot resolution. In summary, the results shown here indicate that detailed observations of geosat glints have the capability of providing significant complementary information beyond that normally obtained from diffuse signatures.

7. ACKNOWLEDGEMENTS

We wish to recognize a number of people who have helped with observing, provided stimulating discussion, or in some other way contributed to this work: L. Bright, S. Gregory, S. Levine, B. O'Neill, S. Restaino, S. Strosahl, T. Tilleman, C. Wilcox, R. Winter, R. Zavala,

8. REFERENCES

1. Vrba, F.J., Fliegel, H.F., and Warner, L.F., Optical Brightness Measurements of GPS Block II, IIA, and IIR Satellites on Orbit, Proceedings 2003 AMOS Technical Conference, 2003.
2. Gregory, S.A., Payne, T.E., and Luu, K. Comparisons Between Simulated and Observed Color Photometric Signatures of Geosynchronous Satellites, Proceedings 2005 AMOS Technical Conference, 146-153, 2005.
3. Chaudahary, A., Birkemeier, C., Gregory, S., Payne, T., and Brown J., Unmixing the Materials and Mechanics Contributions in Non-resolved Object Signatures, Proceedings 2008 AMOS Technical Conference, 381-389, 2008.
4. Payne, T.E., Gregory, S.E., Luu, K., SSA Analysis of GEOS Photometric Signature Classifications and Solar Panel Offsets, Proceedings 2006 AMOS Technical Conference. 667-673, 2006.
5. Payne, T.E., Gregory, S.A., Tombasco, J., Luu, K., and Durr, L., Satellite Monitoring, Change Detection, and Characterization Using Non-Resolved Electro-Optical Data From a Small Aperture Telescope, Proceedings 2007 AMOS Technical Conference, 450-463, 2007.
6. Vrba, F.J., Fliegel, H.F., and Warner, L.F., The Discrimination of GPS Block II, IIA, and IIR Satellites: Spectral Energy Distributions Between 450-2220 NM, Proceedings 2004 AMOS Technical Conference, 64-72, 2004.
7. James, N., Iridium Satellites Light Up the Sky, *J. Brit. Astron.*, 108, 187-188, 1998.
8. Payne, T.E., Gregory, S.A., Vrba, F.J., and Luu, K., Utility of a Multi-Color Photometric Database, Proceedings 2005 AMOS Technical Conference, 137-145, 2005.
9. Armstrong, J.T., et al., The Navy Prototype Optical Interferometer, *Astrophys. J.*, 496, 550-571, 1998.
10. Armstrong, J.T., et al., Observations of a Geosynchronous Satellite With Optical Interferometry, Proceedings 2008 AMOS Technical Conference, 329-336, 2008.
11. Armstrong, J.T., et al., GEO Satellite Imaging at The Naval Prototype Optical Interferometer (NPOI), Proceedings 2009 AMOS Technical Conference, 2009.
12. Hindsley, R., et al. Observations of Geosynchronous Satellites with the Navy Prototype Optical Interferometer, *Appl. Optics* (in preparation), 2009.
13. Landolt, A. U., UBVR Photometric Standard Stars in the Magnitude Range $11.5 < V < 16.0$ Around the Celestial Equator, *Astron J.*, 104, 340-376, 1992.
14. Schaeffer, B. E., et al., The Perseus Flasher and Satellite Glints, *Astrophys. J.*, 320, 398-404, 1987.